

**Valence Transition Theory of the Pressure-Induced  
Dimensionality Crossover in Superconducting  $\text{Sr}_{14-x}\text{Ca}_x\text{Cu}_{24}\text{O}_{41}$**

Jeong-Pil Song

*Department of Physics, University of Arizona Tucson, AZ 85721*

R. Torsten Clay

*Department of Physics and Astronomy and HPC<sup>2</sup> Center for Computational Sciences,  
Mississippi State University, Mississippi State MS 39762*

Sumit Mazumdar

*Department of Physics, University of Arizona, Tucson, AZ 85721*

(Dated: July 5, 2022)

arXiv:2207.00628v1 [cond-mat.str-el] 1 Jul 2022

More than three decades after the discovery of superconductivity (SC) in the cuprates, the nature of the “normal” state and the mechanism of SC remain mysterious. One popular theoretical approach has been to treat the  $\text{CuO}_2$  layer as coupled two-leg one-band Hubbard ladders. In the undoped two-leg ladder spin-singlets occupy ladder rungs, and doped ladders are characterized by superconducting correlations with quasi-long range order (quasi-LRO). Pressure-induced SC in  $\text{Sr}_{14-x}\text{Ca}_x\text{Cu}_{24}\text{O}_{41}$  (SCCO) has long been explained within one-band ladder theories<sup>1,2</sup>. The dramatic pressure-driven crossover from quasi one-to-two dimensional (1D-to-2D) transport<sup>3</sup> and the simultaneous vanishing of the spin gap due to ladder singlets<sup>4,5</sup> in the metallic state preceding SC however lie outside the scope of ladder-based theories<sup>6,7</sup>. Recent demonstration of rapid decay of superconducting correlations with distance within a realistic multiband model of the cuprate ladder<sup>8</sup> gives additional credence to this viewpoint. Here we show that the assumption of pressure-driven increase in hole concentration in the ladders cannot explain the dimensionality crossover. The dimensionality crossover is due to discrete change in Cu-ion ionicity accompanied by transfer of holes from the Cu to O-ions, leading to “negative charge-transfer gap”<sup>9–13</sup>. Our theory of valence transition driven dimensionality crossover in SCCO provides a generic explanation of the very large increase in charge carrier density at critical doping concentrations in both hole<sup>14</sup> and electron<sup>15</sup> doped layered cuprates. We propose a falsifiable experimental test of our theory.

Theoretical efforts to elucidate the mechanism of SC in the cuprates have been overwhelmingly within the one-band Hubbard Hamiltonian. Whether or not the one-band Hamiltonian reproduces the complete physics of the multiband model that explicitly includes both Cu- and O-ions is being increasingly questioned, particularly since the demonstration of nonsuperconducting ground state within the optimally doped purely two-dimensional (2D) Hubbard model<sup>16</sup>. Numerical investigations of SC within single-band Hamiltonians have subsequently focused on models that include the hopping  $t'$  between next nearest neighbor sites<sup>17-20</sup>, or on approaches that treat the one-band 2D lattice as weakly-coupled two-leg ladders<sup>21,22</sup>. Convincing evidence for SC within the 2D Hubbard Hamiltonian with  $t' \neq 0$  is still lacking. Theories based on weakly-coupled one-band Hubbard ladders are considered promising, given the repeated numerical demonstrations of superconducting correlations with quasi-LRO in the two-leg one-band ladder<sup>1,2,23-25</sup>. Experimental observation of SC in  $10 \leq x \leq 13.6$  SCCO<sup>3,6,7,26</sup>, consisting of weakly coupled CuO<sub>2</sub> ladders, has been interpreted as confirmation of the prediction from one-band ladder-based models.

Multiple experimental research groups have maintained that SC in SCCO is 2D, and is likely outside the scope of ladder-based theories. SC in SCCO results not from mere substitution of Sr with Ca in the parent compound Sr<sub>14</sub>Cu<sub>24</sub>O<sub>41</sub>, but is pressure-driven<sup>3,5-7,27</sup>. In the  $x = 11.5$  single crystal SC is realized under pressure  $P = 3.5 - 8$  GPa, with maximum superconducting  $T_c = 9$  K at 4.5 GPa. The ambient pressure resistivity  $\rho_c$  along the ladder leg direction (**c** axis) is metallic at ambient pressure for temperature  $T > 80$  K, but shows an upturn at lower  $T$ . The resistivity  $\rho_a$  along the ladder rung direction (**a** axis) is incoherent even at high  $T$  at ambient pressure, indicating nearly vanishing interladder electronic coupling. This situation changes dramatically for pressure  $P > P_c = 3.5$  GPa, when  $\rho_c$  is metallic at all  $T$ , its magnitude at 300 K nearly one-third of that at ambient pressure. The change in  $\rho_a$  is even more dramatic, with strongly enhanced coherent metallic behavior at all  $T$  for  $P > P_c$ . Importantly,  $\rho_a/\rho_c$  drops by a factor of  $\sim 4-5$  at  $T$  near 50 K, where a maximum in this ratio occurs at ambient pressure. The “average resistivity”  $(\rho_c\rho_a)^{1/2}$  immediately prior to superconducting transition corresponds to the universal 2D resistivity  $h/4e^2$ , confirming further the 2D character of the superconducting transition<sup>3</sup>. As of now there exists no theoretical explanation of the pressure-induced dimensionality crossover preceding SC<sup>3,6</sup>.

Experimental determination of nonzero spin gap for all  $x$  in SCCO<sup>7</sup> is cited in support

of the ladder approach<sup>1,2</sup>. NMR measurements have, however, consistently reported the appearance of gapless spin excitations<sup>4,5,7,27</sup> at the superconducting composition for  $P \geq P_c$ . Pressure-dependent measurement of relaxation time  $T_1$  has shown transition from an activated to Korringa-like behavior at exactly the pressure where there occurs a large jump in the superconducting  $T_c$ <sup>5</sup>. These observations are in strong disagreement with those expected from doped weakly-coupled two-leg ladders. Experimental research groups have conjectured that pressure-driven hole transfer from the  $\text{CuO}_2$  chains to the  $\text{Cu}_2\text{O}_3$  ladders is behind the two-dimensionality and vanishing of the spin gap<sup>6,7,28,29</sup>. The validity of this conjecture remains unclear. Substitution of Sr with Ca may drive hole transfer from the chain to the ladder, but the extent of this transfer appears to be small<sup>30</sup>. More importantly, increased Ca-substitution increases  $\rho_a/\rho_c$ , which appears to contradict the conjecture that increased ladder hole concentration drives two dimensionality<sup>6</sup>.

The need to go beyond ladder theories has been demonstrated even more succinctly in recent Density Matrix Renormalization Group (DMRG) computation of the distance-dependent superconducting pair correlations within a multiband two-leg ladder Hamiltonian containing both Cu- and O-ions<sup>8</sup>. The quasi-LRO found from one-band Hubbard ladder calculations<sup>23-25</sup> is absent in the multiband ladder for realistic Coulomb repulsion of holes on O-ions and O-O hole hopping. As a consequence of the strong pair-breaking effect due to the O-O hopping all conceivable superconducting pair correlations decay rapidly with distance in the multiband ladder<sup>8</sup>.

We report here DMRG calculations of intra- versus interladder coupling strengths for coupled  $\text{Cu}_2\text{O}_3$  ladders within a multiband Hubbard model. The  $90^\circ$  Cu-O-Cu interladder linkage implies that the effective interladder Cu-Cu hopping integral is tiny<sup>6,31</sup>. The absence of noticeable deformation of the ladder structure up to 9 GPa<sup>6</sup> indicates that the interladder Cu-Cu coupling continues to be weak under pressure. Interladder coupling necessarily originates from hole-hopping between O-ions occupying different ladders. The possibility then exists that inclusion of realistic O-O hopping<sup>32</sup> in computations within the multiband coupled-ladder Hamiltonian might indeed find increased two-dimensionality with increased doping. We show conclusively that the assumption of pressure-driven increased hole concentration in the ladders fails to reproduce the observed increase in effective dimensionality. We then show that two-dimensionality can be understood only within a recently proposed valence transition theory of layered cuprates<sup>33</sup>, wherein the insulator-to-conductor transi-

tion is accompanied by a sharp decrease in Cu-ion ionicity from nearly +2 to nearly +1. Nearly all holes, including the ones previously occupying the Cu  $d_{x^2-y^2}$ -orbitals, now occupy the 2D O-sublattice and are charge carriers. The Cu-sublattice with closed shell  $d^{10}$  occupancy plays a secondary role in transport in the metallic state. Valence transition has been widely discussed in the context of neutral-ionic transition in organic charge-transfer solids<sup>34–37</sup> and heavy fermion materials<sup>38–40</sup>. Following valence transition cuprates have negative charge-transfer gap<sup>9–13</sup> meaning that charge-transfer absorption in the ground state involves hole-transfer from the O-anion to the Cu-cation and not the other way around.

### Coupled multiband ladder model

In Fig. 1(a) we show the schematic of the coupled multiband ladders we consider. The Hamiltonian is written as

$$\begin{aligned}
H = & \Delta_{dp} \sum_{\mu,i,\sigma} p_{\mu,i,\sigma}^\dagger p_{\mu,i,\sigma} - \sum_{\mu,\lambda,\langle ij \rangle,\sigma} t_{dp} (d_{\mu,\lambda,i,\sigma}^\dagger p_{\mu,j,\sigma} + H.c.) \\
& - \sum_{\mu,\langle ij \rangle,\sigma} t_{pp} (p_{\mu,i,\sigma}^\dagger p_{\mu,j,\sigma} + H.c.) - \sum_{\mu \neq \mu', \langle ij \rangle,\sigma} t'_{pp} (p_{\mu,i,\sigma}^\dagger p_{\mu',j,\sigma} + H.c.) \\
& + U_d \sum_{\mu,\lambda,i} d_{\mu,\lambda,i,\uparrow}^\dagger d_{\mu,\lambda,i,\uparrow} d_{\mu,\lambda,i,\downarrow}^\dagger d_{\mu,\lambda,i,\downarrow} + U_p \sum_{\mu,j} p_{\mu,j,\uparrow}^\dagger p_{\mu,j,\uparrow} p_{\mu,j,\downarrow}^\dagger p_{\mu,j,\downarrow}. \quad (1)
\end{aligned}$$

Here  $d_{\mu,\lambda,i,\sigma}^\dagger$  creates a hole with spin  $\sigma$  on the  $i$ th Cu  $d_{x^2-y^2}$  orbital on the  $\lambda$ -th leg ( $\lambda = 1, 2$ ) of the  $\mu$ -th ladder ( $\mu = 1, 2$ );  $p_{\mu,j,\sigma}^\dagger$  creates a hole on the rung oxygen O<sub>R</sub> or leg oxygen O<sub>L</sub>;  $t_{dp}$  are nearest neighbor (n.n.) intraladder rung and leg Cu-O hopping integrals, and  $t_{pp}$  and  $t'_{pp}$  are n.n. intra- and interladder O-O hopping integrals, respectively (Fig. 1(a)).  $U_d$  and  $U_p$  are the onsite repulsions on the Cu and O sites. We have chosen  $t_{dp} = 1$ ,  $t_{pp} = 0.5$ ,  $U_d = 8$  and  $U_p = 3$ , based on first principles calculations<sup>32</sup>. We show computational results for two different  $t'_{pp} = 0.3$  and  $0.5$  to demonstrate that our overall conclusion is independent of the choice of  $t'_{pp}$ .

First principles calculations of the parameters in Eq. 1 are performed for parent insulating compounds<sup>32</sup>, and are assumed to be valid in the doped conducting materials. We argue that  $\Delta_{dp}$  is necessarily carrier-concentration dependent<sup>33,41,42</sup>. In order to test ladder-based superconductivity theories we initially choose the same  $\Delta_{dp} = 3$  found by Hirayama *et al.*<sup>32</sup> and used in our single-ladder multiband calculation<sup>8</sup>. This choice is substantiated by our DMRG calculations of the spin gap as a function of  $\Delta_{dp}$  for the single and coupled ladder

systems (Section S.2, Supplementary Information (SI)). The finite-size extrapolated spin gaps are nearly the same for the single and coupled ladders for  $\Delta_{dp} = 2$  and 3, but the spin gap collapses for the coupled ladder for  $\Delta_{dp} = 1$  (Fig. S2).

We measure effective dimensionalities from calculations of n.n. bond orders, which are expectation values of charge-transfers between ions. Bond orders, though not direct measures of d.c. resistivity, measure the electronic kinetic energy in any direction, and are related by sum-rule to the frequency-dependent optical conductivity. We have calculated, (i) n.n. Cu-O bond order  $B_{leg}^{Cu-O}$  along the ladder legs at the interface of the two ladders,  $\langle \sum_{\sigma} d_{\mu,\lambda,i,\sigma}^{\dagger} p_{\mu,j,\sigma} + H.c. \rangle$ , (ii) intra-ladder bond order  $B_{intra}^{O-O}$  between n.n.  $O_R$  and  $O_L$ ,  $\langle \sum_{\sigma} p_{\mu,i,\sigma}^{\dagger} p_{\mu,j,\sigma} + H.c. \rangle$ , and (iii) inter-ladder bond order  $B_{inter}^{O-O}$ ,  $\langle \sum_{\sigma} p_{\mu,i,\sigma}^{\dagger} p_{\mu',j,\sigma} + H.c. \rangle$ , where  $\mu \neq \mu'$  and  $i, j$  are n.n. In addition to n.n. bond orders we have also calculated n.n.n. bond orders along the ladder legs at the interface of the two ladders,  $B_{leg}^{Cu-Cu} = \langle \sum_{\sigma} d_{\mu,\lambda,i,\sigma}^{\dagger} d_{\mu,\lambda,i+1,\sigma} + H.c. \rangle$ , and  $B_{leg}^{O-O} = \langle \sum_{\sigma} p_{\mu,i,\sigma}^{\dagger} p_{\mu,j,\sigma} + H.c. \rangle$ . Our DMRG computations are for coupled ladders consisting of 8 and 12 Cu-O-Cu rungs (hereafter  $8 \times 2$  and  $12 \times 2$  ladders), consisting of 76 and 116 total number of ions, respectively, with open boundary conditions along both ladder leg and rung directions (*Methods*). Bond orders being local two-fermion operators exhibit negligible finite size effects (see Table II and Fig. S4 in SI for size-dependence of bond orders at  $U_d = U_p = 0$ , where convergence is slowest)

## Doping dependence of dimensionality

We first test the conjecture that increase in effective dimensionality is a consequence of hole transfer from chains to ladders<sup>6,7,28,29</sup>. We report computational results for different dopings  $\delta$ , where  $1 + \delta$  is the average hole concentration per Cu-ion ( $\delta = 0$  for the undoped ladders). In Fig. 2 we have shown calculated bond orders within Eq. 1 for the  $8 \times 2$  coupled ladder system, for fixed  $\Delta_{dp} = 3$ .  $B_{leg}^{Cu-O}$  and  $B_{intra}^{O-O}$ , taken together (but not simply additively) is a measure of intraladder hole transport, while  $B_{inter}^{O-O}$  is the measure of interladder transport. The increases in intraladder bond orders  $B_{leg}^{Cu-O}$ ,  $B_{intra}^{O-O}$ ,  $B_{leg}^{Cu-Cu}$  and  $B_{leg}^{O-O}$  with  $\delta$ , though still small, are relatively more significant. The overall computational results are in strong agreement with the conclusion in reference 6, viz., increased  $\delta$  increases anisotropy, and not otherwise. The very large pressure-driven decrease<sup>3</sup> in  $\rho_a/\rho_c$  at low T thus cannot be understood within the hole-transfer conjecture<sup>6,7,28,29</sup>.

An interesting feature in Fig. 2 is the very large  $B_{intra}^{O-O}$  relative to  $B_{inter}^{O-O}$ , for both  $t'_{pp}$ .

It is tempting to assign this larger magnitude to simply the additional paths via Cu-ions that holes can take when hopping from  $O_L$ -to- $O_R$  of the same ladder that are not available to holes hopping between interladder  $O_L$  ions. The additional O-O hole hopping integrals are  $\sim t_{dp}^2/\Delta_{dp}$  and  $t_{dp}^2/(U_d + \Delta_{dp})$ , respectively, which are both smaller than  $t'_{pp}$ . Strictly from consideration of the magnitudes of the hopping integrals,  $B_{intra}^{O-O}$  should have been closer to  $B_{inter}^{O-O}$  than found in Fig. 2, and hole transport in SCCO should have been far less anisotropic even at ambient pressure. In Figs. 1(b) and 1(c) we have given the schematics of the intraladder  $O_R$ -to- $O_L$  hole transfers, involving and not involving the hole on the Cu-ion, respectively. The much larger calculated  $B_{intra}^{O-O}$  in Fig. 2 implies that hole transfers via paths in Fig. 1(b) dominate overwhelmingly over the path in Fig. 1(c). Bond orders and the true interladder coupling strengths therefore depend not only on the magnitudes of the hopping integrals, but also on the effective charges on the ions involved. In Table III (SI) we have given the Cu- and O-ion charges for two  $t'_{pp}$  and different  $\delta$ . The very small O-ion charges for  $\Delta_{dp} = 3$  explain the small magnitudes of  $B_{inter}^{O-O}$ .

## Valence transition

It follows that two dimensionality requires substantial increase in hole population on the O-sublattice, which is intrinsically 2D unlike the Cu-sublattice. Large increase in O-ion hole occupancy can only originate from significant change in  $\Delta_{dp}$ , including even change of sign which would correspond to transition from positive to negative charge-transfer gap. Negative charge-transfer gap has been computationally found in several different materials, based largely on extensions to Density Functional Theory (DFT)<sup>9-13</sup>. Here we approach it from the ionic limit, which allows easier visualization of the boundary between positive and negative charge-transfer<sup>34,35</sup>. Negative charge-transfer requires that the key transition metal cation M can exist in two stable proximate oxidation states, usually  $M^{n+}$  and  $M^{(n-1)+}$ , with the true ionicity given by the inequality<sup>33</sup>,

$$I_n + A_2 + \Delta E_{M,n} + \Delta(W) \gtrsim 0 \quad (2)$$

where  $I_n$  is  $n$ th ionization of M ( $M^{(n-1)+} \rightarrow M^{n+} + e$ ) and  $A_2$  is the second electron-affinity of O.  $\Delta E_{M,n} = E_{M,n} - E_{M,n-1}$ , where  $E_{M,n}$  and  $E_{M,n-1}$  are the per cation Madelung energies of the solid with the cation charges of  $+n$  and  $+(n-1)$ , respectively.  $\Delta(W) = W_n - W_{n-1}$ , where  $W_n$  and  $W_{n-1}$  are the per cation gains in one-electron delocalization (band) energies

of states with cationic charges  $+n$  and  $+(n-1)$ , respectively. Larger right hand (left hand) side favors  $M^{n+}$  ( $M^{(n-1)+}$ ) with positive (negative) charge-transfer gap. Distinct near-integer oxidation states, as opposed to mixed valence requires that the two largest terms in Eq. 2,  $I_n$  and  $|\Delta E_{M,n}|$  are much larger than  $|t_{dp}|$ , even as the overall charge-transfer gap is comparable to  $|t_{dp}|$ .

$I_n$  and  $A_2$  are both positive, and often only the large gain in Madelung energy  $\Delta E_{M,n}$  drives larger cationic charge  $M^{n+}$ . The tendency to negative charge-transfer gap is strongest for ions with unusually large  $I_n$ . The latter is a characteristic of  $M^{(n-1)+}$  ions with electron configurations that are completely closed-shell or exactly half-filled, modulo crystal field stabilization (section S.5.1, SI). Within the valence transition theory, SCCO at ambient pressures is correctly described within the standard picture of weakly coupled two-leg ladders with  $\text{Cu}^{2+}$ -ions at the vertices and positive  $\Delta_{dp}$ . The  $\mathbf{a}$ -axis resistivity is incoherent because of the very small density of holes on O-sites. The system is however close to the boundary between positive and negative charge-transfer gap defined by Eq. 2 because of large  $I_2$  (section S.5.1, SI). Pressure brings  $\text{CuO}_2$  chain and  $\text{Cu}_2\text{O}_3$  ladder layers, both of which contain excess holes, closer to one another. The resultant increase in electrostatic repulsion decreases  $|\Delta E_{M,n}|$  and drives the transition from positive to negative charge-transfer.  $\Delta(W)$  stabilizes the metallic state with negative charge-transfer further. The argument for negative charge-transfer gap in  $\text{CrO}_2$ , where however the metallicity is due to self-doping<sup>9</sup>, is very similar.

### Dimensionality crossover following valence transition

We show that the assumption of pressure-driven valence transition successfully explains the observed dimensionality crossover. In Fig. 3(a) we have plotted the same bond orders as in Fig. 2, for  $12 \times 2$  coupled ladders, now as a function of  $\Delta_{dp}$  for fixed  $\delta = 0.125$ , for  $t'_{pp} = 0.5$ . These results are in sharp contrast with those of Fig. 2.  $B_{leg}^{Cu-O}$ ,  $B_{intra}^{O-O}$  and  $B_{inter}^{O-O}$  all increase as  $\Delta_{dp}$  goes from positive to negative, simulating the decrease of  $\rho_c$  and  $\rho_a$  with pressure. For each  $\Delta_{dp}$  we have also calculated the charge densities  $\langle n_{Cu} \rangle$ ,  $\langle n_{OR} \rangle$  and  $\langle n_{OL} \rangle$  (see Table IV, SI). In Fig. 3(b) we have plotted the ratios of the interladder coupling  $B_{inter}^{O-O}$  with  $B_{leg}^{Cu-O}$ ,  $B_{intra}^{O-O}$  and  $B_{leg}^{O-O}$  against  $\langle n_{OL} \rangle$  at different  $\Delta_{dp}$ , for comparison against the pressure dependence of  $\rho_a/\rho_c$ . Increasing  $B_{inter}^{O-O}/B_{leg}^{Cu-O}$  and  $B_{inter}^{O-O}/B_{intra}^{O-O}$  with increasing  $\langle n_{OL} \rangle$  does simulate the decreasing  $\rho_a/\rho_c$  with pressure<sup>3</sup>. The increases are small within

the positive  $\Delta_{dp}$  region (see Table I, SI) compared to the factor of 4-5 decrease in  $\rho_a/\rho_c$  in SCCO between ambient pressure and  $P = 3.5\text{-}4.5$  GPa at  $T \sim 50$  K. Thus  $B_{inter}^{O-O}/B_{leg}^{Cu-O}$  at  $\Delta_{dp} = 1$  is larger by only a factor of  $\sim 1.75$  relative to its magnitude at  $\Delta_{dp} = 3$ . The increase in  $B_{inter}^{O-O}/B_{intra}^{O-O}$  is larger by a factor of 1.42. The corresponding increases relative to  $\Delta_{dp} = 3$ , are larger by factors of  $\sim 3.0$  and  $\sim 1.9$ , respectively, at  $\Delta_{dp} = -1$  and  $\sim 4.70$  and  $\sim 2.45$  at  $\Delta_{dp} = -2$  (Table I in SI). Figs. S7(a) and (b) (SI) show the corresponding plots for  $t'_{pp} = 0.3$ . The behavior are very similar to those in Figs. 3(a) and (b), with all bond order ratios at  $t'_{pp} = 0.3$  and 0.5 very close to one another (Table I, SI). We conclude that the large decrease in  $\rho_a/\rho_c$  necessarily requires transition from positive to negative  $\Delta_{dp}$ . The simultaneous changes in the slopes in all three ratios at  $\Delta_{dp} = -1$  is a signature of discrete jump in Cu-ion ionicity.

The valence transition model at first glance may come across as too exotic to be relevant to real cuprates. The point remains, however, that rigorous quantum computations have so far failed to find long range superconducting correlations within the standard models for cuprates that treat them as weakly doped Mott insulators. Especially in view of the recent demonstration of the absence of superconducting correlations with quasi-LRO within the multiband Hubbard ladder<sup>8</sup>, it has become essential to reexamine the fundamental hypotheses behind the standard approaches. As shown here, the crossover from incoherent-to-coherent  $\rho_a$ , universal two-dimensional resistivity<sup>3</sup> and gapless spin excitations<sup>4,5,7,27</sup> in the pressure-driven metallic state preceding SC are all expected within the valence transition theory. As discussed in section S.5.2 (SI), assumption of Cu-ion charge of  $\sim +(1.0\text{--}1.2)$  following valence transition gives a charge of  $\sim -(1.4\text{--}1.45)$  on the O-anions, very close to charge  $-1.5$  in the negative charge-transfer compound  $\text{FeO}_2$ <sup>11</sup>. Our theory provides a unified mechanism for the large jump in the number of charge carriers at critical doping concentrations in both hole<sup>14</sup> and electron<sup>15</sup>-doped layered cuprates. Entirely holelike charge carriers in the latter<sup>15</sup> agrees with our assertion that transport in this region is due to hole hopping among the O-ions only and the nearly closed-shell Cu-ions play a subsidiary role. It has been hypothesized that SC in cuprates emerges from the strange metallic state reached at the quantum critical points, and characterized by large number of carriers<sup>14,15</sup>. Our previous theoretical work demonstrating the enhancement of superconducting correlations by Hubbard  $U$  uniquely in the frustrated strongly correlated  $\frac{1}{4}$ -filled band<sup>43,44</sup> is in agreement with this hypothesis. We end this work with an experimental prediction, viz., that pressure-

dependent Hall coefficient measurements in SCCO will find a large jump in the number of charge carriers beyond  $P_c$ , exactly as in the layered systems beyond critical doping<sup>14,15</sup>.

- 
- <sup>1</sup> E. Dagotto. Experiments on ladders reveal a complex interplay between a spin-gapped normal state and superconductivity. *Rep. Prog. Phys.*, 62:1525, 1999.
  - <sup>2</sup> K. Le Hur and T. M. Rice. Superconductivity close to the Mott state: From condensed-matter systems to the superfluidity in optical lattices. *Ann. Phys.*, 324:1452–1515, 2009.
  - <sup>3</sup> T. Nagata, M. Uehara, J. Goto, J. Akimitsu, N. Motoyama, H. Eisaki, S. Uchida, H. Takahashi, T. Nakanishi, and N. Mori. Pressure-induced dimensional crossover and superconductivity in the hole-doped two-leg ladder compound  $\text{Sr}_{14-x}\text{Ca}_x\text{Cu}_{24}\text{O}_{41}$ . *Phys. Rev. Lett.*, 81:1090–1093, 1998.
  - <sup>4</sup> H. Mayaffre, P. Auban-Senzier, M. Nardone, D. Jérôme, D. Poilblanc, C. Bourbonnais, U. Ammerahl, G. Dhahenne, and A. Revcolevschi. Absence of a spin gap in the superconducting ladder compound  $\text{Sr}_2\text{Ca}_{12}\text{Cu}_{24}\text{O}_{41}$ . *Science*, 279:345–348, 1998.
  - <sup>5</sup> N. Fujiwara, Y. Fujimaki, S. Uchida, K. Matsubayashi, T. Matsumoto, and Y. Uwatoko. NMR and NQR study of pressure-induced superconductivity and the origin of critical-temperature enhancement in the spin-ladder cuprate  $\text{Sr}_2\text{Ca}_{12}\text{Cu}_{24}\text{O}_{41}$ . *Phys. Rev. B*, 80:100503(R), 2009.
  - <sup>6</sup> K. M. Kojima, N. Motoyama, H. Eisaki, and S. Uchida. The electronic properties of cuprate ladder materials. *J. Electron Spectroscopy and Related Phenomena*, 117-118:237–250, 2001.
  - <sup>7</sup> T. Vuletić, B. Korin-Hamzić, T. Ivek, S. Tomić, B. Gorshunov M. Dressel, and J. Akimitsu. The spin-ladder and spin-chain system  $(\text{La},\text{Y},\text{Sr},\text{Ca})_{14}\text{Cu}_{24}\text{O}_{41}$ : Electronic phases, charge and spin dynamics. *Phys. Rep.*, 428:169–258, 2006.
  - <sup>8</sup> J.-P. Song, S. Mazumdar, and R. T. Clay. Absence of Luther-Emery superconducting phase in the three-band model for cuprate ladders. *Phys. Rev. B*, 104:104504, 2021.
  - <sup>9</sup> A. Korotin, V. I. Anisimov, D. I. Khomskii, and G. A. Sawatzky.  $\text{CrO}_2$ : a self-doped double exchange ferromagnet. *Phys. Rev. Lett.*, 80:4305–4308, 1998.
  - <sup>10</sup> S. S. Streltsov, A. O. Shorikov, S. L. Skornyakov, A. I. Poteryaev, and D. I. Khomskii. Unexpected 3+ valence of iron in  $\text{FeO}_2$ , a geologically important material lying “in between” oxides and peroxides. *Sci. Rep.*, 7:13005, 2017.
  - <sup>11</sup> E. Koemets et al. Revealing the complex nature of bonding in the binary high-pressure com-

- pound FeO<sub>2</sub>. *Phys. Rev. Lett.*, 126:106001, 2021.
- <sup>12</sup> A. Khazraie, K. Foyevtsova, I. Elfimov, and G. A. Sawatzky. Oxygen holes and hybridization in the bismuthates. *Phys. Rev. B*, 97:075103, 2018.
- <sup>13</sup> M. Chandler Bennett, G. Hu, G. Wang, O. Heinonen, P. R. C. Kent, J. T. Kroge, and P. Ganesh. Origin of metal-insulator transitions in correlated perovskite metals. *Phys. Rev. Research*, 4:L022005, 2022.
- <sup>14</sup> C. Proust and L. Taillefer. The remarkable underlying ground states of cuprate superconductors. *Ann. Rev. Condens. Matter Phys.*, 10:409–429, 2019.
- <sup>15</sup> R. L. Greene, P. R. Mandal, N. R. Poniatowski, and T. Sarkar. The strange metal state of the electron-doped cuprates. *Ann. Rev. Condens. Matter Phys.*, 11:213–229, 2020.
- <sup>16</sup> M. Qin, C.-M. Chung, H. Shi, E. Vitali, C. Hubig, U. Schollwöck, S. R. White, and S. Zhang. Absence of superconductivity in the pure two-dimensional Hubbard model. *Phys. Rev. X*, 10:031016, 2020.
- <sup>17</sup> B.-X. Zheng, C.-M. Chung, P. Corboz, G. Ehlers, M.-P. Qin, R. M. Noack, H. Shi, S. R. White, S. Zhang, and G. K.-L. Chan. Stripe order in the underdoped region of the two-dimensional Hubbard model. *Science*, 358:1155–1160, 2017.
- <sup>18</sup> H. C. Jiang and T. P. Devereaux. Superconductivity in the doped Hubbard model and its interplay with next nearest hopping  $t'$ . *Science*, 365:1424–1428, 2019.
- <sup>19</sup> C.-M. Chung, M. Qin, S. Zhang, U. Schollwöck, and S. R. White. Plaquette versus ordinary  $d$ -wave pairing in the  $t'$ -Hubbard model on a width 4 cylinder. *Phys. Rev. B*, 102:041106(R), 2020.
- <sup>20</sup> S. Jiang, D. J. Scalapino, and S. R. White. Ground-state phase diagram of the  $t - t' - J$  model. *Proceedings of the National Academy of Sciences of the USA*, 118:e2109978118, 2021.
- <sup>21</sup> Y. Gannot, Y.-F. Jiang, and S. A. Kivelson. Hubbard ladders at small  $U$  revisited. *Phys. Rev. B*, 102:115136, 2020.
- <sup>22</sup> H.-C. Jiang and S. A. Kivelson. Stripe order enhanced superconductivity in the Hubbard model. *Proceedings of the National Academy of Sciences of the USA*, 119:e2109406119, 2022.
- <sup>23</sup> E. Dagotto, J. Riera, and D. Scalapino. Superconductivity in ladders and coupled planes. *Phys. Rev. B*, 45:5744–5747, 1992.
- <sup>24</sup> R. M. Noack, N. Bulut, D. J. Scalapino, and M. G. Zacher. Enhanced  $d_{x^2-y^2}$  pairing correlations in the two-leg Hubbard ladder. *Phys. Rev. B*, 56:7162, 1997.

- <sup>25</sup> M. Dolfi, B. Bauer, S. Keller, and M. Troyer. Pair correlations in doped Hubbard ladders. *Phys. Rev. B*, 92:195139, 2015.
- <sup>26</sup> M. Uehara, T. Nagata, J. Akimitsu, H. Takahashi, N. Mori, and K. Kinoshita. Superconductivity in the ladder material  $\text{Sr}_{0.4}\text{Ca}_{13.6}\text{Cu}_{24}\text{O}_{41.84}$ . *J. Phys. Soc. Jpn.*, 65:2764–2767, 1996.
- <sup>27</sup> N. Fujiwara, N. Mori, Y. Uwatoko, T. Matsumoto, N. Motoyama, and S. Uchida. Superconductivity of the  $\text{Sr}_2\text{Ca}_{12}\text{Cu}_{24}\text{O}_{41}$  spin-ladder system: Are the superconducting pairing and the spin-gap formation of the same origin? *Phys. Rev. Lett.*, 90:137001, 2003.
- <sup>28</sup> M. Isobe, T. Ohta, M. Onoda, F. Izumi, S. Nakano, J. Q. Li, Y. Matsui, E. Takayama-Muromachi, T. Matsumoto, and H. Hayakawa. Structural and electrical properties under high pressure for the superconducting spin-ladder system  $\text{Sr}_{0.4}\text{Ca}_{13.6}\text{Cu}_{24}\text{O}_{41+\delta}$ . *Phys. Rev. B*, 57:613–621, 1998.
- <sup>29</sup> Y. Piskunov, D. Jérôme, P. Auban-Senzier, P. Wzietek, and A. Yakubovskiy. Hole redistribution in  $\text{Sr}_{14-x}\text{Ca}_x\text{Cu}_{24}\text{O}_{41}$  ( $x=0,12$ ) spin ladder compounds:  $^{63}\text{Cu}$  and  $^{17}\text{O}$  NMR studies under pressure. *Phys. Rev. B*, 72:064512, 2005.
- <sup>30</sup> M. Bugnet, S. Loeffler, D. Hawthorn, H. A. Dabkowska, G. M. Luke, P. Schattschneider, G. A. Sawatzky, G. Radtke, and G. A. Botton. Real-space localization and quantification of hole distribution in chain-ladder  $\text{Sr}_3\text{Ca}_{11}\text{Cu}_{24}\text{O}_{41}$  superconductor. *Sci. Adv.*, 2:e1501652, 2016.
- <sup>31</sup> T. F. A. Müller, V. Anisimov, T. M. Rice, I. Dasgupta, and T. Saha-Dasgupta. Electronic structure of ladder cuprates. *Phys. Rev. B*, 57:R12655–R12688, 1998.
- <sup>32</sup> M. Hirayama, Y. Yamaji, T. Misawa, and M. Imada. Ab initio effective Hamiltonians for cuprate superconductors. *Phys. Rev. B*, 98:134501, 2018.
- <sup>33</sup> S. Mazumdar. Valence transition model of the pseudogap, charge order, and superconductivity in electron-doped and hole-doped copper oxides. *Phys. Rev. B*, 98:205153, 2018.
- <sup>34</sup> J. B. Torrance, J. E. Vazquez, J. J. Mayerle, and V. Y. Lee. Discovery of a neutral-to-ionic phase transition in organic materials. *Phys. Rev. Lett.*, 46:253–257, 1981.
- <sup>35</sup> J. B. Torrance, A. Girlando, J. J. Mayerle, J. I. Crowley, V. Y. Lee, and P. Batail. Anomalous nature of neutral-to-ionic phase transition in tetrathiafulvalene-chloranil. *Phys. Rev. Lett.*, 47:1747–1750, 1981.
- <sup>36</sup> S. Koshihara, Y. Tokura, T. Mitani, G. Saito, and T. Koda. Photoinduced valence instability in the organic molecular compound tetrathiafulvalene-p-chloranil (TTF-CA). *Phys. Rev. B*, 42:6853–6856, 1990.

- <sup>37</sup> M. Masino, N. Castagnetti, and A. Girlando. Phenomenology of the neutral-ionic valence instability in mixed stack charge-transfer crystals. *Crystals*, 7:108, 2017. and references therein.
- <sup>38</sup> I. Felner and I. Nowik. First-order valence phase transition in cubic  $\text{Yb}_x\text{In}_{1-x}\text{Cu}_2$ . *Phys. Rev. B*, 33:617–619, 1986.
- <sup>39</sup> C. Dallera, M. Grioni, A. Shukla, G. Vanko, J. L. Sarrao, J. P. Rueff, and D. L. Cox. New spectroscopy solves an old puzzle: The kondo scale in heavy fermions. *Phys. Rev. Lett.*, 88:196403, 2002.
- <sup>40</sup> K. Miyake. New trend of superconductivity in strongly correlated electron systems. *J. Phys.: Condens. Matter*, 19:125201, 2007.
- <sup>41</sup> J. E. Hirsch. Effect of orbital relaxation on the band structure of cuprate superconductors and implications for the superconductivity mechanism. *Phys. Rev. B*, 90:184515, 2014.
- <sup>42</sup> N. Barisic and D. K. Sunko. High- $T_c$  cuprates: a story of two electronic subsystems. *Journal of Superconductivity and Novel Magnetism*, 2022.
- <sup>43</sup> N. Gomes, W. Wasanthi De Silva, T. Dutta, R. T. Clay, and S. Mazumdar. Coulomb enhanced superconducting pair correlations in the frustrated quarter-filled band. *Phys. Rev. B*, 93:165110, 2016.
- <sup>44</sup> W. Wasanthi De Silva, N. Gomes, S. Mazumdar, and R. T. Clay. Coulomb enhancement of superconducting pair-pair correlations in a  $\frac{3}{4}$ -filled model for  $\kappa$ -(BEDT-TTF) $_2$ X. *Phys. Rev. B*, 93:205111, 2016.
- <sup>45</sup> Matthew Fishman, Steven R. White, and E. Miles Stoudenmire. The ITensor software library for tensor network calculations. <https://arxiv.org/abs/2007.14822>, 2020.
- <sup>46</sup> E. M. Stoudenmire and S. R. White. Real-space parallel density matrix renormalization group. *Phys. Rev. B*, 87:155137, 2013.

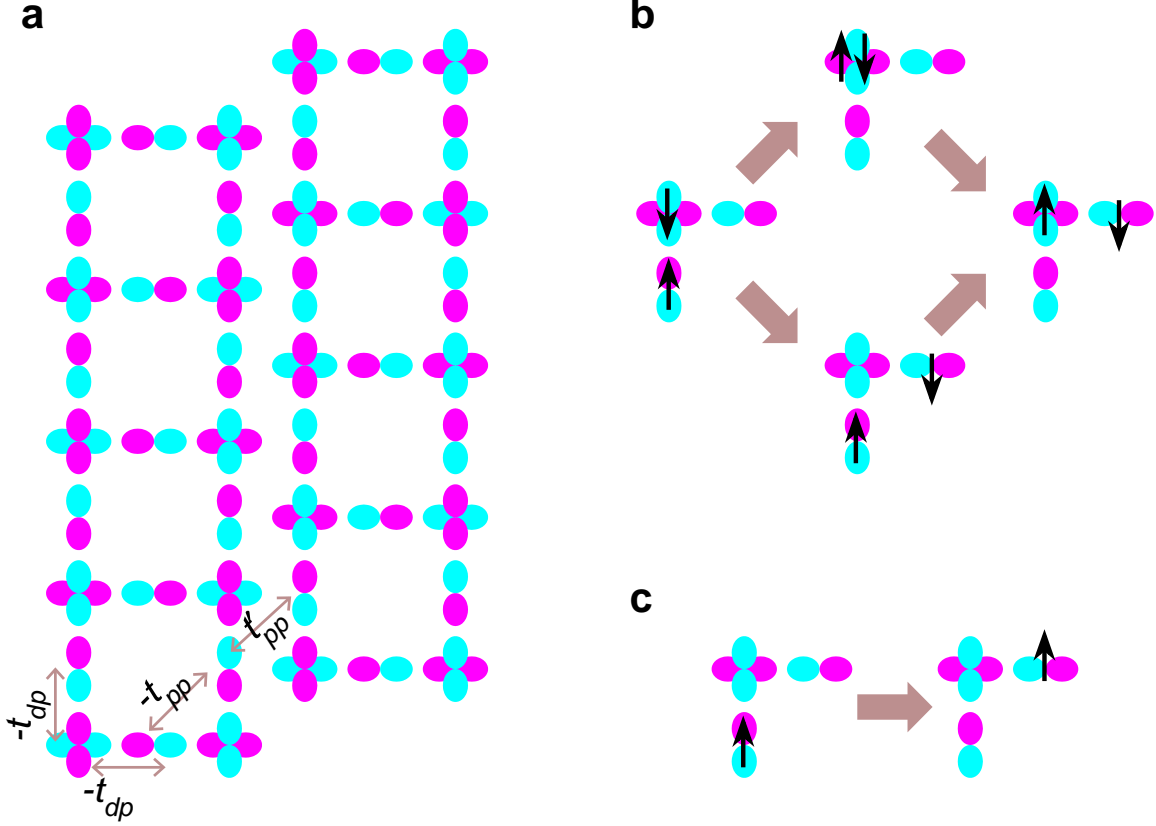


FIG. 1:  $L \times 2$  coupled multiband ladder. **a.** Schematic of the coupled two-leg multiband  $\text{Cu}_2\text{O}_3$  ladders investigated numerically. The actual calculations are for  $8 \times 2$  and  $12 \times 2$  ladders, where the first number denotes the number of Cu-O-Cu rungs in each ladder. The total number of ions included in the calculations are 76 and 116, respectively. The intraladder hopping parameters  $t_{dp}$  and  $t_{pp}$ , and the interladder hopping  $t'_{pp}$  are indicated in the figure. **b.** Intraladder hole hopping between leg oxygen  $O_L$  and rung  $O_R$  at ambient pressure involving the hole on the Cu-ion. **c.** Direct intraladder hole hoppings between O-ions without involving the hole on the Cu-ion. The hole occupancy of the Cu-ion in this case is irrelevant.

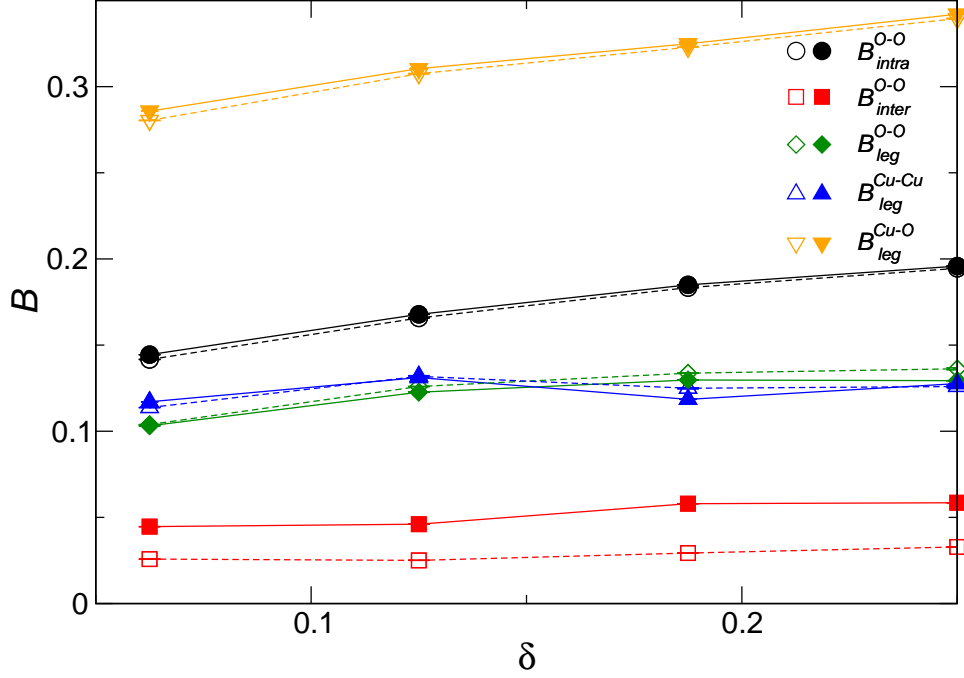


FIG. 2: Interladder coupling as a function of doping. Calculated bond orders  $B$  (see text) for  $\Delta_{dp} = 3$  versus hole doping  $\delta$ . Solid and dashed curves correspond to  $t'_{pp} = 0.5$  and  $0.3$ , respectively. The calculations are for the  $8 \times 2$  coupled ladders. There is no indication of increasing two-dimensionality with  $\delta$  for either  $t'_{pp}$ .

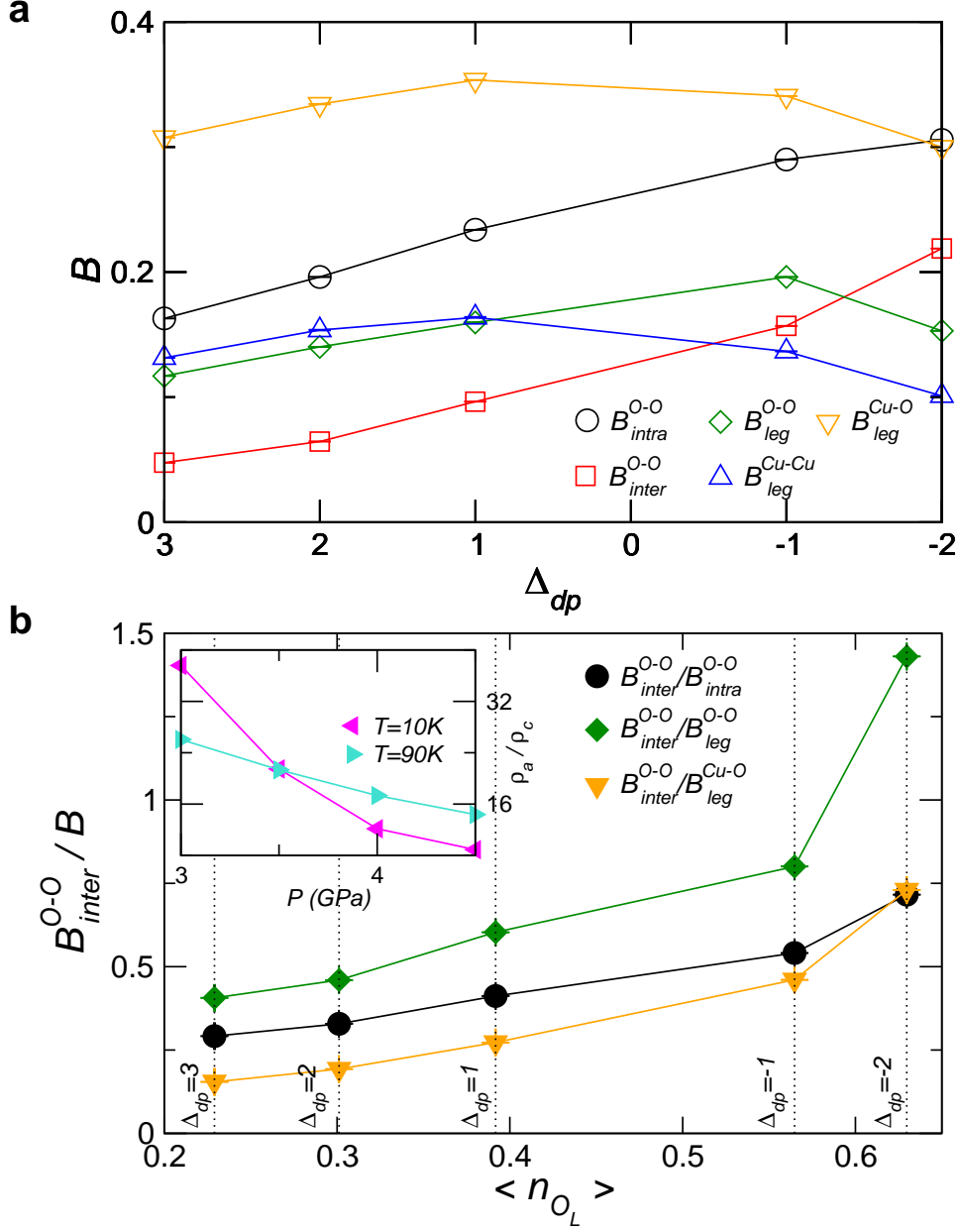


FIG. 3: Interladder coupling versus charge-transfer gap. **a** Calculated bond orders for fixed  $\delta = 0.125$  versus  $\Delta_{dp}$ , for  $t'_{pp} = 0.5$ . **b**. Ratios of interladder bond order with all intraladder bond orders, versus hole density on the oxygen ions occupying the interior legs of the coupled ladder. The  $\Delta_{dp}$  corresponding to each data point is indicated on the figure. Calculations are for the  $12 \times 2$  coupled ladder, the largest system we have studied. The computational results for  $t'_{pp} = 0.3$  are nearly identical and are shown in Figure S7(a) and (b). Inset shows the ratio of resistivity along the ladder rung to that along the ladder leg direction at two different temperatures, obtained from data points in Reference 3.

**Methods** Our DMRG calculations were done with open boundary conditions with Cu-O-Cu rungs at both ends (see Fig. 1). Calculations used the ITensor library<sup>45</sup> with a two-site DMRG update and particle number and  $S_z$  conservation, and were parallelized using the method of Reference 46. We considered coupled ladders of up to  $16 \times 2$  rungs (156 sites) in the undoped case, and  $12 \times 2$  rungs (116 sites) in the doped case, with DMRG bond dimension  $m$  of up to 13000. Because of the open boundary conditions at the ends of the ladders, the charge density and bond orders vary with position along the length of each ladder. For the values we report for the bond orders, we averaged over all bonds of the same type, excluding bonds directly connected to the outer boundaries. For charge densities we averaged over all Cu,  $O_R$  and  $O_L$  sites. We extrapolated energies and correlation functions to zero truncation error as detailed in the Supplementary Information.

**Acknowledgments** Work at Arizona was supported by National Science Foundation (NSF) grant NSF-CHE-1764152. Some calculations in this work were supported under project TG-DMR190068 of the Extreme Science and Engineering Discovery Environment (XSEDE), which is supported by National Science Foundation grant number ACI-1548562. Specifically, we used the Bridges2 system at the Pittsburgh Supercomputing Center, which is supported by NSF award ACI-1928147.

**Author contributions** SM and RTC conceived of the project. JPS performed the DMRG calculations. RTC developed the DMRG codes. SM wrote the manuscript. All authors participated in analyzing data from the calculations.

**Competing interests** The authors declare no competing interests.

**Supplementary Information** Please see the attached PDF file.